

Vibrational excitation of the electronic ground state of H₂ via electron-impact excitation and radiative decay

L H Scarlett¹, J K Tapley¹, D V Fursa¹, J S Savage¹, M C Zammit², and I Bray¹

¹*Department of Physics and Astronomy, Curtin University, Perth, Western Australia, Australia*

²*Theoretical Division, Los Alamos National Laboratory, Los Alamos, New Mexico, USA*

Electron-impact excitation and dissociation of molecules is an important process which plays a major role in governing the dynamics of astrophysical, industrial, and fusion plasmas. The H₂ molecule is a significant species in many plasma environments, particularly in the divertor region of tokamak reactors, where more than 90% of the neutral hydrogen is molecular [1]. In the divertor region many of these H₂ molecules are present in vibrationally excited states. The cross sections for excitation and dissociation of vibrationally-excited H₂ are substantially larger than for H₂ in the ground vibrational level. Therefore a careful analysis of processes in fusion plasma requires detailed information on the vibrational distribution of molecular hydrogen. The purpose of this work is to present a new set of reliable cross sections for producing vibrationally-excited H₂ via electron-impact processes. The full details are presented in Ref. [2].

Above the first electronic-inelastic threshold, the dominant pathway to producing vibrationally-excited H₂ in plasmas is excitation-radiative-decay (ERD) - the radiative decay to bound vibrational levels of the ground electronic state after electron-impact transitions to electronic singlet states. Cross sections for this process are important for accurate modelling of hydrogenic plasmas where H₂ is present in a range of vibrational levels. Excitation-radiative-decay dissociation (ERDD) occurs when excited singlet states decay radiatively into the dissociative vibrational continuum of the ground state. This process is one of the dominant mechanisms for dissociation of H₂, with important implications for modelling fusion and astrophysical plasmas.

A theoretical approach to modelling the ERD and ERDD processes requires detailed information on vibrationally-resolved electron-impact excitations for a large number of electronically excited states. The majority of theoretical work in determining ERD and ERDD cross sections for e⁻-H₂ collisions has been performed using the semi-classical impact-parameter (IP) method [3, 4]. The IP results for excitation cross sections are up to a factor of two larger than the available measurements for low- to intermediate-energy electrons scattering on the ground vibrational level, and are likely to be similarly inaccurate for scattering on excited levels.

More recently our group has extended the convergent close-coupling method to electron collisions with molecular hydrogen [5, 6]. The CCC approach [7] starts with the fixed-nuclei (FN) formulation where the total wave function is expanded in a complete set of N target-state func-

tions represented in spheroidal coordinates [8]. The scattering-system time-independent electronic Schrödinger equation is transformed into the momentum-space coupled-channel Lippmann-Schwinger equation for the T matrix. Projectile wave functions are expanded in partial waves to reduce the equations in three dimension to effectively one dimension. FN partial-wave scattering amplitudes and cross sections are obtained over a range of internuclear separations. Increasing the target-state expansion size and the size of the projectile partial-wave expansion leads to converged cross sections.

In the adiabatic-nuclei (AN) method the FN partial-wave scattering amplitudes calculated at incident energy E and internuclear distance R $F_{f\lambda_f m_f, i\lambda_i m_i}(R, E)$ are utilized to obtain cross sections for vibrational excitations $iv_i \rightarrow fv_f$:

$$\sigma_{fv_f, iv_i} = \frac{q_{fv_f}}{q_{iv_i}} \sum_{\lambda_f m_f \lambda_i m_i} \left| \langle \chi_{fv_f} | F_{f\lambda_f m_f, i\lambda_i m_i} | \chi_{iv_i} \rangle \right|^2 \quad (1)$$

Vibrational wave functions $\chi_{nv_n}(R)$ are obtained by diagonalising the Born-Oppenheimer molecular Hamiltonian. The ERD and ERDD cross sections are calculated in the following way,

$$\sigma_{iv_i', f, iv_i}^{\text{ERD}} = \sum_{v_f} \frac{A_{i,f}(v_i', v_f)}{A_f(v_f)} \sigma_{fv_f, iv_i}, \quad (2)$$

$$\sigma_{iv_i', f, iv_i}^{\text{ERDD}} = \sum_{v_f} \sigma_{fv_f, iv_i} - \sum_{v_i'} \sigma_{iv_i', f, iv_i}^{\text{ERD}} \quad (3)$$

where $A_{i,f}(v_i', v_f)$ is the $fv_f \rightarrow iv_i'$ radiative transition probability and $A_f(v_f)$ is the total transition probability for the fv_f state. The summations are taken over all bound vibrational levels of the corresponding electronic states.

The spheroidal-coordinate formulation of the CCC method allows for an accurate representation of target wave functions over a large range of internuclear distances as illustrated in Fig. 1. This is important for accurate evaluation of the integral over R in Eq. (1). The first six singlet excited states shown in Fig. 1 contribute between 80% (for scattering on $v_i = 14$) and 95% ($v_i = 0$) of the ERD and ERDD cross sections. The present calculations have been performed in two models. The 210-state model is labelled CCC-S(210) and accounts for excitations of both bound and continuum part of the H_2 spectrum. The testing we have done indicates that this model produces convergent cross sections for the transitions of interest in this work.

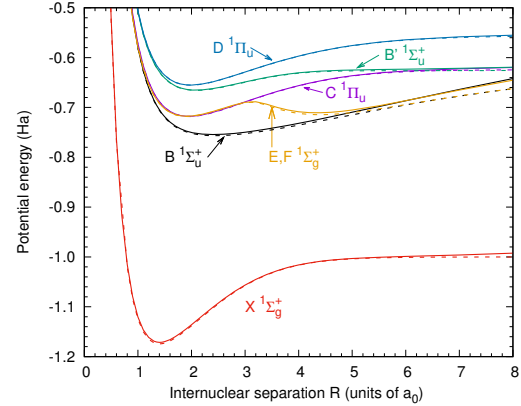


Figure 1: Potential-energy curves for the first six singlet states of H_2 .

The second model has 27 states which account only for reaction channels leading to bound spectrum excitations. This model is labelled CC(27).

In Fig. 2 we present the ERD cross section summed over excitations to the $B^1\Sigma_u^+$, $C^1\Pi_u$, $B'^1\Sigma_u^+$, $D^1\Pi_u$, and $E, F^1\Sigma_g^+$ states for a selection of v_i . These include scattering from the $v_i = 0, 5$ and 10 levels to all final vibrational levels. Radiative decays from the excited states shown in Fig. 1 are treated explicitly using Eq. (2), with an estimate made for the contribution from the remaining singlets. In each case, the cross section is largest for decays back to the same initial vibrational level ($v_i' = v_i$) and decreases for increasing $|v_i - v_i'|$. This behaviour has also been observed in Refs. [3, 9].

For comparison with Celiberto *et al* [3] and Hiskes [9], we present ERD cross sections for scattering on the ground vibrational state summed over excitations via the $B^1\Sigma_u^+$ and $C^1\Pi_u$ states in Fig. 3. Here we also compare the CC(27) and CCC-S(210) scattering models. The CCC-S(210) and CC(27) results are in agreement with each other and with the IP cross sections in the high energy region where they are expected to converge to the first-Born approximation results. As the IP formulation is a high energy approximation and describes the projectile motion classically, it is not expected to produce accurate results at intermediate to threshold energies. This is reflected in the disagreement of the IP results with both Hiskes [9] and CCC-S(210), where the IP results are greater by up to a factor of 2. The CC(27) model neglects coupling to the target electronic continuum, resulting in larger cross sections in the intermediate energy region as flux is redistributed to the bound electronic channels. We note that the CCC-S(210) cross sections are in good agreement with Hiskes [9] where available, and within the $^{+20}_{-30}\%$ uncertainty quoted by Hiskes [9] for the maximum.

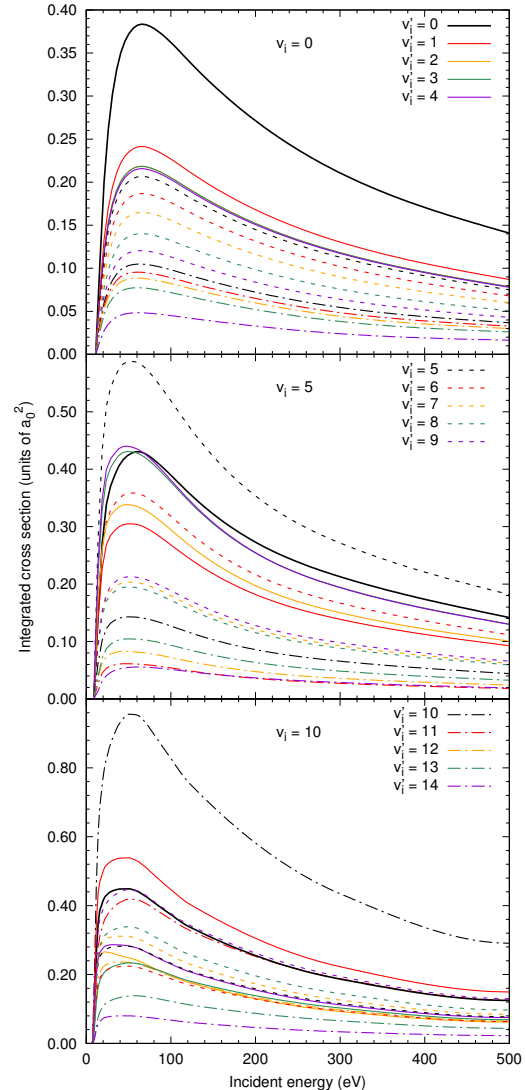


Figure 2: ERD cross sections for scattering on the $v_i = 0, 5$, and 10 vibrational levels of the $X^1\Sigma_g^+$ state, leading to excitation of the singlet spectrum and radiative decay to the bound $v_i' = 0 - 14$ levels of the $X^1\Sigma_g^+$ state.

In Fig. 4 we compare the CCC cross sections with the IP calculations of Celiberto *et al* [4], who presented ERDD cross sections summed over the $B^1\Sigma_u^+$ and $C^1\Pi_u$ state contributions only. For all vibrational levels, the $B^1\Sigma_u^+$ and $C^1\Pi_u$ combined ERDD cross section comprises 85–95% of the total ERDD cross section. As seen in Fig. 4, the CCC ERDD cross sections are up to factor of two lower than the IP results at low to intermediate energies, however both calculations are in excellent agreement at higher energies.

In conclusion, we have presented electron-impact excitation-radiative-decay (ERD) and ERD dissociation (ERDD) cross sections for scattering on the $X^1\Sigma_g^+(v_i = 0 - 14)$ levels via excitation of the singlet states of H_2 with full details presented in Ref. [2]. The ERD cross sections are in good agreement with the calculations of Hiskes [9], where available, but in significant disagreement with the more comprehensive IP calculations [3, 4] except at high energies where the IP formalism becomes valid. The level of agreement with the IP results is the same for the ERDD cross sections.

References

- [1] K. Sawada, T. Fujimoto, *J. Appl. Phys.* **78**, 2913 (1995).
- [2] L. H. Scarlett, J. K. Tapley, J. S. Savage, D. V. Fursa, M. C. Zammit, I. Bray, *Plasma Sources Sci. Technol.* **28**, 025004 (2019)
- [3] R. Celiberto, M. Capitelli, U. T. Lamanna *Chem. Phys.* **183**, 101 (1994)
- [4] R. Celiberto, U. T. Lamanna, M. Capitelli, *Phys. Rev. A* **50**, 4778 (1994)
- [5] M. C. Zammit, J. S. Savage, D. V. Fursa and I. Bray, *Phys. Rev. Lett.* **116**, 233201 (2016)
- [6] M. C. Zammit, J. S. Savage, D. V. Fursa, I. Bray, *Phys. Rev. A* **95**, 022708 (2017).
- [7] M. C. Zammit *et. al.*, M. C. Zammit, J. S. Savage, D. V. Fursa, I. Bray, *J. Phys. B: Atom. Molec. Phys.* **50**, 123001 (2017).
- [8] J. K. Tapley, L. H. Scarlett, J. S. Savage, M. C. Zammit, D. V. Fursa, I. Bray, *J. Phys. B At. Mol. Phys.* **51**, 144007 (2018).
- [9] J. R. Hiskes, *J. Appl. Phys.* **7**, 3409 (1991)

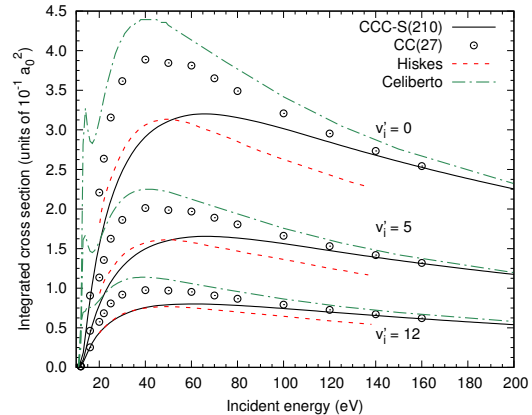


Figure 3: Cross sections for ERD via the $B^1\Sigma_u^+$ and $C^1\Pi_u$ states, for scattering on the $v_i = 0$ level of the $X^1\Sigma_g^+$ state. 27-state and 210-state CCC results for decays to the $v'_i = 0, 5$, and 10 levels are compared with the previous calculations of Celiberto *et al.* [3] and Hiskes [9].

Integrated cross section (units of $10^{-1} a_0^2$)

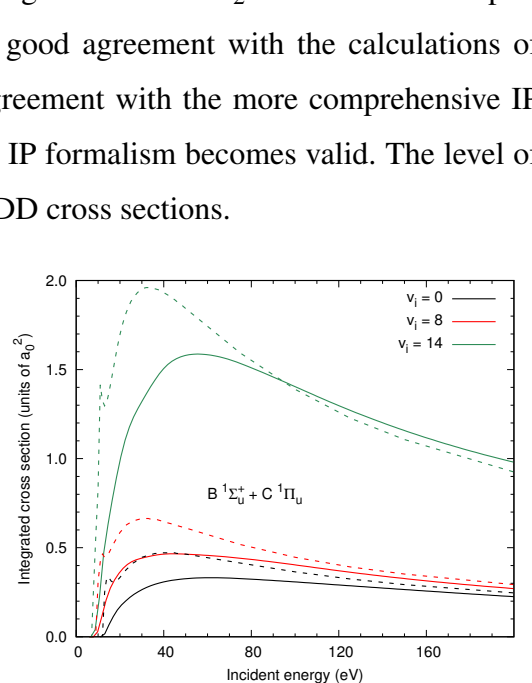


Figure 4: Sum of the present $B^1\Sigma_u^+$ and $C^1\Pi_u$ excitation-radiative-decay dissociation cross sections (solid lines) compared with the impact-parameter calculations of Celiberto et al [4] (dashed lines).

Integrated cross section (units of a_0^2)